

Systematic variation of the electronic structure of 3d transition-metal compounds

T. Saitoh, A. E. Bocquet, T. Mizokawa, and A. Fujimori
Department of Physics, University of Tokyo, Bunkyo-ku, Tokyo 113, Japan
 (Received 17 March 1995)

We have studied the systematic changes of the electronic structure in 3d transition-metal oxides and sulfides within a configuration-interaction cluster model including multiplet effects. Parameters of the model have been deduced from analyses of the 2p core-level photoemission spectra of these compounds. We have calculated the magnitudes of the band gaps, the net *d*-electron numbers, and the character of doped carriers (and hence of band gaps) within the cluster model. The variation of the calculated magnitudes of the band gaps is in good agreement with experiment, especially with those derived in a recent optical study by Arima *et al.* of the LaMO₃ series, where *M* denotes a transition-metal element.

I. INTRODUCTION

3d transition-metal (TM) compounds have attracted much interest due to their variety of magnetic, electrical, and structural properties. In many of these compounds, conventional band-structure calculations¹ fail to explain experimental results, especially the opening of the large band gaps. Also, satellite structures that appear in the core-level and valence-band photoemission spectra cannot be explained by these calculations. The satellite structures reflect many-body effects arising from electron-electron interaction and TM 3d-ligand *p* orbital hybridization. Therefore, by analyzing these structures one can obtain much information on the electronic states of these compounds. Because the conventional band picture breaks down, many photoemission spectra have been analyzed using a configuration-interaction (CI) cluster-model approach.² Based on the results of the photoemission studies, a framework for the 3d TM compounds, the so-called Zaanen-Sawatzky-Allen (ZSA) scheme, is formulated.^{3,4} According to this scheme, the compounds can be classified into the Mott-Hubbard regime and the charge-transfer (CT) regime depending on the relative size of the ligand *p*-to-TM 3d charge-transfer energy Δ and the on-site *d*-*d* Coulomb repulsion energy *U*.

In previous papers, we have investigated a number of 3d TM compounds by analyzing the TM 2p core-level photoemission spectra and identified the systematic change of Δ and *U* as functions of the TM atomic number and valence including the effects of *d*-*d* multiplet splitting in the framework of the CI cluster model.^{5,6} A similar systematic variation of Δ and *U* has been found for TM halides by Okada, Kotani, and Thole.⁷ In this paper, we present results for the calculated variations of the band gaps, the net *d*-electron numbers, and the character of doped carriers,⁸ and discuss the systematic change of the electronic structure of 3d TM oxides and sulfides including lighter TM oxides. For the band gaps of the LaMO₃ series, where *M* denotes a TM element, our results are compared with a recent optical study by Arima, Tokura, and Torrance.⁹ A brief account of the present work has been reported in Ref. 8.

II. CONFIGURATION-INTERACTION CLUSTER MODEL

In the TM compounds studied here, the TM ions are octahedrally coordinated by ligand anions,¹⁰ and, therefore, the fivefold degenerate 3d orbitals are split into triply degenerate *t*_{2g} and doubly degenerate *e*_g orbitals. Hence, in order to calculate the electronic structures of the TM compounds, we have considered an octahedral cluster $[M^{k+}(O^{2-})_6]^{-(12-k)}$, where *k* + is the valence of the TM ion. The ground state is described as

$$\Psi_g = a_n |d^n\rangle + a_{n+1} |d^{n+1}\underline{L}\rangle + \cdots + a_{10} |d^{10}\underline{L}^{10-n}\rangle, \quad (1)$$

where *n* denotes the nominal 3d electron number and \underline{L} is a ligand hole. As most of the compounds studied here are insulators, our cluster-model calculations, which determine the local electronic structure, are considered to be a good starting point.

The model is described by three parameters, namely, the multiplet-averaged *d*-*d* Coulomb interaction *U*, the ligand *p*-to-TM *d* charge-transfer energy Δ and the ligand *p*-TM *d* transfer integral (*pd* σ). We have adjusted the

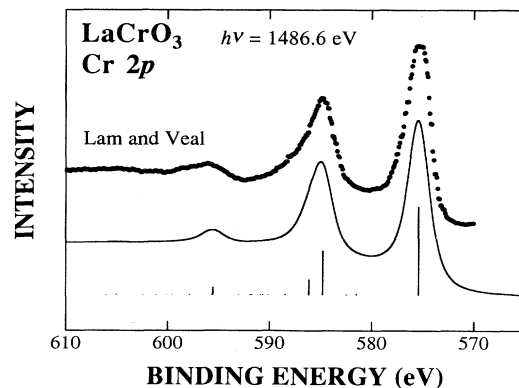


FIG. 1. Cluster-model analysis of the Cr 2p spectra of LaCrO₃. The calculated spectrum (solid line) is compared with the experimental spectrum by Lam and Veal (Ref. 12) (dots).

parameters so as to fit the calculated spectra to the experimental TM $2p$ core-level data. An example of the analyses is shown in Fig. 1 for LaCrO_3 . We have calculated the band gap E_{gap} , the net d -electron number $N_d(n)$, and the character of doped carriers C_{hole}^p , C_{electron}^d . The definitions of these quantities are

$$E_{\text{gap}} \equiv E(n+1) + E(n-1) - 2E(n), \quad (2)$$

$$N_d(n) \equiv n|a_n|^2 + (n+1)|a_{n+1}|^2 + \dots + 10|a_{10}|^2, \quad (3)$$

$$C_{\text{hole}}^p \equiv 1 - [N_d(n) - N_d(n-1)], \quad (4)$$

$$C_{\text{electron}}^d \equiv N_d(n+1) - N_d(n).$$

Details of the calculations are described in Refs. 5, 6, 8, and 11.

III. RESULTS

As already discussed in previous papers,^{5,6} Δ and U represent the smooth variation of the electronic structure of TM compounds as a function of the TM atomic number and valence. The Δ , U , and $(pd\sigma)$ values used in the present work are listed in Table I. Δ increases in going from Co to Ti reflecting the changes in the electronegativities of the metal ions. U decreases with decreasing TM atomic number due to the increase in the spatial extent of the d orbitals, although its change is weak. We can also define Δ_{eff} and U_{eff} , respectively, as the ligand p -to-TM d charge-transfer energy and the d - d Coulomb interaction with respect to the lowest energies of the multiplets.⁶ Observed physical properties are more directly related to Δ_{eff} and U_{eff} rather than to Δ and U : Δ_{eff} and U_{eff} show nonmonotonic variations as functions of the atomic number and valence due to the nonmonotonic behavior of

TABLE I. Δ , U , and $(pd\sigma)$ values used in the present work (in eV). The values in parentheses are extrapolated from the late TM monoxides.

Compound	Δ	U	$(pd\sigma)$
LaTiO_3	6.0	4.0	-2.4
LaCrO_3	5.2	5.2	-1.9
LaMnO_3	4.5	7.5	-1.8
LaFeO_3	2.5	7.5	-1.4
LaCoO_3	2.0	5.5	-1.7
SrMnO_3	2.0	7.8	-1.5
SrFeO_3	0.0	7.8	-1.3
(TiO)	(8.0)	(5.0)	(-1.3)
(VO)	(7.5)	(5.5)	(-1.2)
(CrO)	(7.0)	(6.0)	(-1.2)
MnO	6.5	7.0	-1.1
FeO	6.0	7.0	-1.1
NiO	4.5	7.5	-1.3
Cr_2O_3	5.2	5.2	-2.0
$\text{Mn}_{0.25}\text{TiS}_2$	4.0	5.4	-0.9
$\text{Fe}_{0.33}\text{TiS}_2$	3.5	5.5	-1.1
$\text{Ni}_{0.33}\text{TiS}_2$	2.5	6.0	-1.3
$\text{Zn}_{0.5}\text{Mn}_{0.5}\text{S}$	4.0	5.8	-1.0
NiS	2.5	5.5	-1.2

the multiplet splitting as a function of n .⁶ The magnitude of $(pd\sigma)$ increases with decreasing n due to the increase in the spatial extent of the d orbitals.

Figure 2 shows the variation of Δ_{eff} and U_{eff} plotted against the $3d$ electron number n . In the present work, we have added data points compared to Refs. 5, 6, and 8 for LaTiO_3 ($n=1$) and LaCrO_3 ($n=3$) by analyzing the TM $2p$ core-level x-ray photoemission spectroscopy spectra reported by Lam and Veal.¹² We have also added Cr_2O_3 ($n=3$).¹³ Figure 2(a) clearly demonstrates that Δ_{eff} decreases monotonically with n except for the large discontinuity between $n=4$ and 5. This variation reflects both the smooth change of Δ and its "multiplet correction," $\Delta_{\text{eff}} - \Delta$, which is a large negative value for $n=4$ and a large positive value for $n=5$.⁶ One can also see that Δ_{eff} (and hence Δ) of those compounds having the same nominal d -electron number decreases, as the valence of TM increases reflecting the decrease in the $3d$ energy level due to the increasing positive charges at the TM ions. Figure 2(b) shows that U_{eff} slowly and mono-

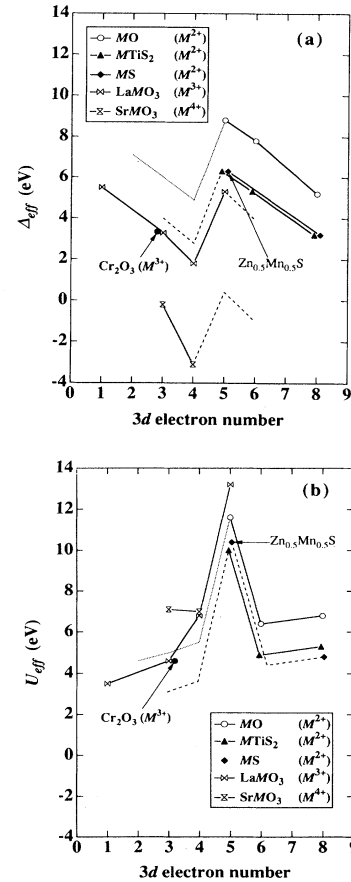


FIG. 2. Effective charge-transfer energy Δ_{eff} (a) and effective averaged $3d$ - $3d$ Coulomb repulsion energy U_{eff} (b) are plotted against the $3d$ -electron number n . Dotted line in MO is deduced from the extrapolated values of Δ and U for MO (see Table I). Dashed lines represent behaviors expected from the systematic variation of the parameters.

tonically increases with n except for the sharp peak at $n=5$. The results for light TM compounds follow the trend that U_{eff} (and U) decreases with decreasing TM atomic number, which was proposed in previous work.^{6,8}

The most remarkable result is the variation of the band gap E_{gap} plotted against n as shown in Fig. 3(a). Besides the data points listed above, LaCoO_3 ($n=6$) is added in this figure¹⁴ and hence we can view the variation of the band gaps for LaMO_3 from Ti to Co. Here it should be noted that LaCoO_3 has a low-spin (1A_1) ground state and shows a gradual transition from the nonmagnetic to a paramagnetic state with increasing temperature.¹⁵ Although the origin of this transition has not yet been understood, we have performed our calculations for the low-spin state because our photoemission spectra have been taken at liquid-nitrogen temperature, i.e., below the transition temperature.¹⁶ Comparing Fig. 3(a) with Fig. 2, the variation of the band gaps reflects that of both Δ_{eff} and U_{eff} . Because of the p - d hybridization, the amount of the variation is weaker than that of Δ_{eff} or U_{eff} . Also,

even for a negative Δ_{eff} value, a finite gap opens (SrMnO_3). Again one can see that the gap shows a sharp peak at $n=5$ corresponding to the peak in Δ_{eff} and U_{eff} , due to the strong Hund's rule-coupling stabilization in the d^5 configuration. At $n=3$, there is another peak that is smaller than that of $n=5$. It also comes from the stabilization due to Hund's rule-coupling because the t_{2g} orbitals are half-filled by the three electrons.

Recently, Arima, Tokura, and Torrance⁹ have studied the optical spectra of LaMO_3 and YMO_3 for a series of $3d$ TM atoms M . In the optical conductivity spectra, they have identified the optical gaps, with which we can compare our calculated values for LaMO_3 . The optically determined CT gap shown in Fig. 3(b) monotonically decreases with the atomic number of M except for the increase in going from Mn ($n=4$) to Fe ($n=5$). This variation is, therefore, essentially the same as that of Δ_{eff} shown in Fig. 2(a). The minimum (actual) optical gaps (either CT-type or Mott-Hubbard-type) of LaMO_3 are also plotted against the atomic number of M in Fig. 3(b). The minimum gaps have two peaks at Cr ($n=3$) and Fe ($n=5$) corresponding to the peaks in Fig. 3(a), except that the optically determined CT gap of LaCrO_3 is larger than that of LaFeO_3 . Considering the different strengths of the Hund's rule-coupling stabilization in the d^3 and d^5 configurations, the gap of LaCrO_3 must be smaller than that of LaFeO_3 . Indeed, the activation energy of LaFeO_3 is so large that one cannot properly measure the resistivity of this compound.¹⁷ The calculated gap for LaTiO_3 is significantly larger than the observed one. This is partly because the gap of the cluster model corresponds to the peak-to-peak separation in the combined photoemission and inverse photoemission spectra, while the optical gap corresponds to the separation between the band edges and hence is smaller than the peak-to-peak separation by the d -band width.

The net d -electron numbers N_d are shown in Fig. 4 as the deviation from the nominal $3d$ electron numbers n . One can see again the effect of the strong Hund's rule-coupling stabilization in the d^5 configuration: When $n=5$, the strongest stabilization is expected and hence the deviation from the nominal configuration is very small. Small shoulders at $n=3$ in the MO and LaMO_3 curves are also due to the half-filled stabilization of the t_{2g} orbitals. The figure shows that as the valence of the TM increases, the $N_d(n)-n$ for a fixed n increases because Δ_{eff} decreases and hence the hybridization strength increases with the TM valence. The M^{4+} compounds show a different behavior from the others. This comes from the fact that Δ_{eff} goes from nearly zero (SrMnO_3) to negative (SrFeO_3). When Δ_{eff} becomes negative, the dominant configuration in the ground state changes from d^n to $d^{n+1}\bar{L}$, resulting in a large $N_d(n)$. The figure also shows that the variation of $N_d(n)-n$ with n becomes stronger as one goes from the $2+$ to $3+$ series. This is not only because the Δ_{eff} values are smaller for the $3+$ oxides than for the $2+$ oxides but also because we find the $(pd\sigma)$ values to be larger for the TM perovskites than for the TM monoxides. The large $N_d(n)-n$ values for light TM compounds are due not

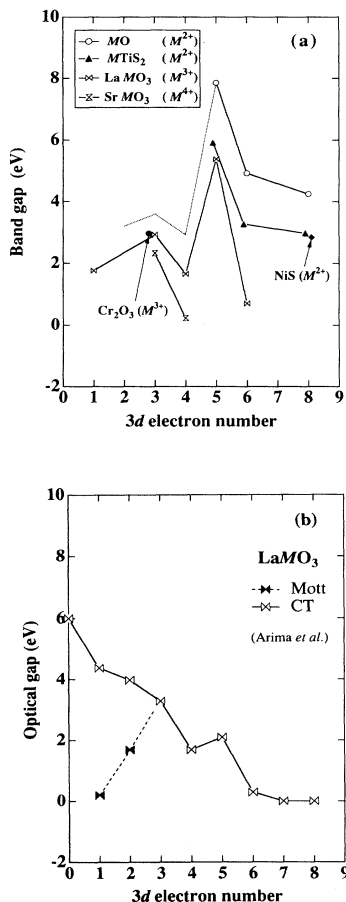


FIG. 3. (a) Calculated band gaps E_{gap} . Dotted line in MO represents the calculated results using the extrapolated values of Δ and U for MO . (b) Observed optical gaps for the LaMO_3 series by Arima, Tokura, and Torrance (Ref. 9).

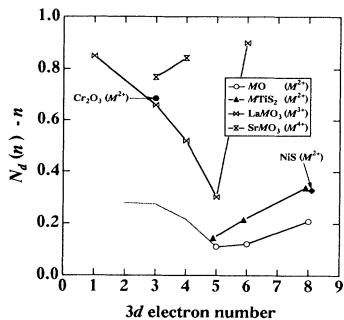


FIG. 4. Deviations of the net d -electron number from the nominal one, $N_d(n) - n$, plotted against the $3d$ -electron number n . Dotted line in MO represents the calculated results using the extrapolated values of Δ and U for MO.

only to the large ($pd\sigma$) values but also to the large number of empty d orbitals into which charge transfer occurs from the occupied ligand p orbitals.¹⁸

Note that our calculation for LaCoO_3 has been performed for the low-spin state. $N_d(n)$ of the low-spin state is larger than that of the high-spin state because the low-spin state has empty e_g orbitals, and the hybridization of the e_g orbitals is larger than that of t_{2g} orbitals. For the high-spin state, we have estimated $N_d(n)$ to be 6.6, which would result in a weaker variation with n .

For the investigation of carrier doping in so-called valence-control compounds, we can obtain important information as to whether the doped carriers occupy the TM d or anion p orbitals. In Fig. 5(a), the p character of the doped holes C_{hole}^p is shown. It generally increases with n , reflecting the decrease in Δ . One can also see that the p character slightly increases with the valence of TM, due to the decrease in Δ . The curves have a peak at $n = 5$ and a dip at $n = 6$ because of the multiplet effect or the Hund's rule coupling. In our previous paper, we have pointed out that $(U_{\text{eff}} - U) - (\Delta_{\text{eff}} - \Delta)$ is a rough measure for the p character of the doped holes.⁶ Indeed, the curves in Fig. 5(a) follow the variation of $(U_{\text{eff}} - U) - (\Delta_{\text{eff}} - \Delta)$ shown in Fig. 5 of Ref. 6.

In Fig. 5(b), the d character of doped electrons C_{electron}^d are plotted against n . The Hund's rule-coupling stabilization and hence the weak covalency in the d^5 configurations enhances the d character of the doped electron. Here one can also see that the d character decreases with the valence of the TM, reflecting the decrease in Δ with the valence of the TM. There are some irregular behaviors in the curves of LaMO_3 ($\text{LaFeO}_3 \rightarrow \text{LaCoO}_3$) and SrMO_3 . This is because the small (LaCoO_3) or negative (SrFeO_3) values of Δ_{eff} make the d character of the doped electrons small. In the case of LaCoO_3 , its low-spin configuration further reduces the d character. For the high-spin state, we have estimated the d character to be about 0.64.

Now we discuss the character of the band gaps from C_{hole}^p and C_{electron}^d . It is widely accepted that one can categorize insulating $3d$ TM compounds into the Mott-

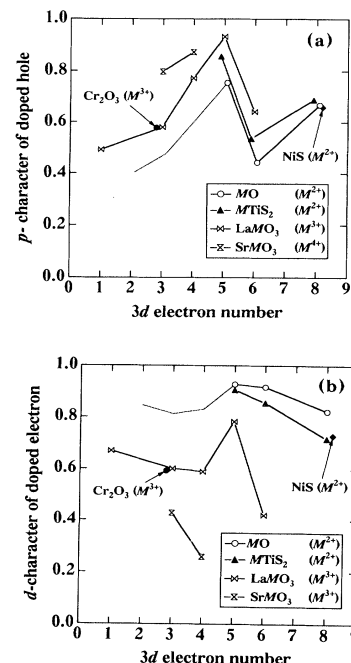


FIG. 5. (a) p character of the doped hole C_{hole}^p . (b) d character of the doped electron C_{electron}^d . Dotted line in MO represents the calculated results using the extrapolated values of Δ and U for MO.

Hubbard-type and the CT-type. In general, early TM compounds, which have $d-d$ gaps, belong to the former type, and late TM compounds, which have $p-d$ gaps, belong to the latter type. In terms of the ZSA diagram,³ the gap is of the $d-d$ type when $U_{\text{eff}} < \Delta_{\text{eff}}$, and of the $p-d$ type when $U_{\text{eff}} > \Delta_{\text{eff}}$. However, it should be noted that the hybridization effect is not explicitly considered in the original classification of ZSA. Our results indicate that the hybridization has a considerable effect on the classification scheme particularly for lighter TM oxides. In our definition, those compounds which have C_{hole}^p smaller than 0.5 and C_{electron}^d larger than 0.5 have $d-d$ gaps, while those compounds which have C_{hole}^p larger than 0.5 and C_{electron}^d larger than 0.5 have $p-d$ gaps. The general variation of the character of the band gaps with n is the same as what is now accepted by many researchers. However, SrMnO_3 , SrFeO_3 , and LaCoO_3 do not have $d-d$ gaps, nor $p-d$ gaps, but $p-p$ gaps.^{11, 16, 19, 20} [In fact, SrFeO_3 is metallic and the calculated gap is also nearly zero.²⁰] In these compounds, strong hybridization effects due to the small Δ_{eff} , the relatively large ($pd\sigma$), and the large number of empty d orbitals contribute to the gap formation. Combining Figs. 5(a) and 5(b), we may plot a diagram similar to that of ZSA as shown in Fig. 6, where we also locate the $p-p$ gap compounds in our diagram. In order to clarify the three regimes, $d-d$, $p-d$, and $p-p$ gaps, the character of the doped carriers is used for the two axes.

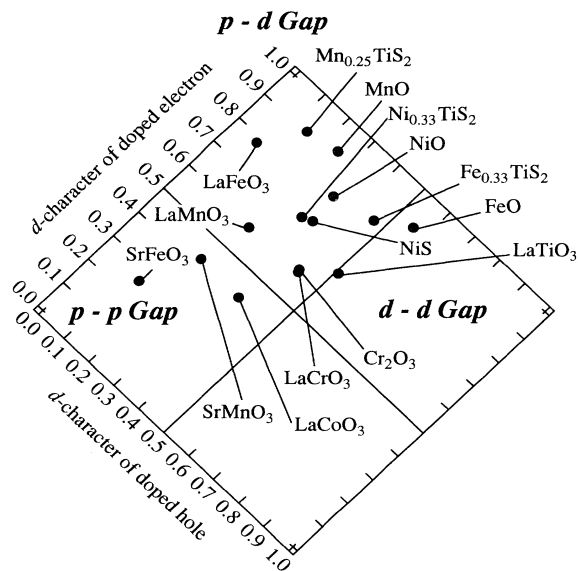


FIG. 6. Character of doped carriers plotted in a two-dimensional diagram. According to this, the characters of the band gaps are classified into the d - d , p - d , and p - p gap.

IV. CONCLUSIONS

We have studied the systematic chemical trends and the multiplet effects on the electronic structure of $3d$ TM oxides and sulfides within the CI cluster model by extending our previous work.^{5,6,8} The band gaps, the net d -

electron numbers and the characters of doped carriers (and hence of band gaps) have been calculated. We have shown that the Hund's rule-coupling stabilization and the p - d hybridization strongly affect the electronic structure of $3d$ TM compounds. The Hund's rule effect dramatically manifests itself in nominally d^5 compounds: Larger band gaps open and the chemical bonding becomes more ionic. This is the main reason why many d^5 compounds are large-gap CT-type insulators. Hybridization effects play an important role in the high-valence, late TM compounds. Because the early TM compounds have large ($pd\sigma$) as well as a large number of empty d orbitals, hybridization effects are also large, reflecting the large deviations of the net d -electron numbers from the nominal ones. The variation of the calculated band gaps with n for the $LaMO_3$ series shows good agreement with that of the observed optical gaps,⁹ indicating that the electronic structure of a wide range of $3d$ TM compounds (especially of insulators) can be basically understood using the CI cluster-model approach.

ACKNOWLEDGMENTS

We would like to thank Dr. T. Arima for useful discussions. All the calculations were performed using a VAX/VMS system at the Meson Science Laboratory, Faculty of Science, University of Tokyo. The present work was supported by a Grant-in-Aid for Scientific Research from the Ministry of Education, Science and Culture and the New Energy and Industrial Technology Development Organization (NEDO). T.S. and A.E.B. are supported by fellowships from the Japan Society for the Promotion of Science.

¹L. F. Mattheiss, Phys. Rev. B **5**, 290 (1972).

²A. Fujimori and F. Minami, Phys. Rev. B **30**, 957 (1984); H. Eskes, L. H. Tjeng, and G. A. Sawatzky, *ibid.* **41**, 288 (1990); J. Ghijsen, L. H. Tjeng, H. Eskes, G. A. Sawatzky, and R. L. Johnson, *ibid.* **42**, 2268 (1990); A. Fujimori, N. Kimizuka, T. Akahane, T. Chiba, S. Kimura, F. Minami, K. Siratori, M. Taniguchi, S. Ogawa, and S. Suga, *ibid.* **42**, 7580 (1990).

³J. Zaanen, G. A. Sawatzky, and J. W. Allen, Phys. Rev. Lett. **55**, 418 (1985); J. Zaanen and G. A. Sawatzky, Can. J. Phys. **65**, 1262 (1987).

⁴S. Hüfner, Z. Phys. B **61**, 135 (1985).

⁵A. E. Bocquet, T. Mizokawa, T. Saitoh, H. Namatame, and A. Fujimori, Phys. Rev. B **46**, 3771 (1992); A. E. Bocquet, T. Saitoh, T. Mizokawa, and A. Fujimori, Solid State Commun. **83**, 11 (1992).

⁶A. Fujimori, A. E. Bocquet, T. Saitoh, and T. Mizokawa, J. Electron Spectrosc. Relat. Phenom. **62**, 141 (1993).

⁷K. Okada, A. Kotani, and B. T. Thole, J. Electron Spectrosc. Relat. Phenom. **58**, 325 (1992).

⁸A. Fujimori, T. Saitoh, T. Mizokawa, and A. E. Bocquet, Jpn. J. Appl. Phys. **32**, Suppl. **32-3**, 217 (1994).

⁹T. Arima, Y. Tokura, and J. B. Torrance, Phys. Rev. B **48**, 17006 (1993).

¹⁰Because the Mn ion in $Zn_{0.5}Mn_{0.5}S$ is tetrahedrally coordinated to four S ligands, only the values of Δ (Δ_{eff}), U (U_{eff}), and ($pd\sigma$) are shown.

¹¹T. Saitoh, A. E. Bocquet, T. Mizokawa, H. Namatame, A. Fujimori, M. Abbate, Y. Takeda, and M. Takano, Phys. Rev. B **51**, 13942 (1995).

¹²D. J. Lam and B. W. Veal, Phys. Rev. B **22**, 5730 (1980).

¹³X. Li, V. E. Henrich, T. Saitoh and A. Fujimori, in *Applications of Synchrotron Radiation Techniques to Materials Science*, edited by D. L. Perry, N. Shinn, R. Stockbauer, K. D'Amico, and L. Termillo, MRS Symposia Proceedings No. 307 (Materials Research Society, Pittsburgh, 1993), p. 205.

¹⁴We do not show the points for $LaCoO_3$ in Fig. 2 because Δ_{eff} and U_{eff} are not meaningful for low-spin compounds.

¹⁵M. Abbate, R. Potze, G. A. Sawatzky, and A. Fujimori, Phys. Rev. B **49**, 7210 (1994); K. Asai, O. Yokokura, N. Nishimori, H. Chou, J. M. Tranquada, G. Shirane, S. Higuchi, Y. Okajima, and K. Kohn, *ibid.* **50**, 3025 (1994); M. Itoh, I. Natori, S. Kubota, and K. Motoya, J. Phys. Soc. Jpn. **63**, 1486 (1994).

¹⁶T. Saitoh *et al.* (unpublished).

¹⁷S. K. Park (private communication).

¹⁸K. Okada, T. Uozumi, and A. Kotani, J. Phys. Soc. Jpn. **63**, 3176 (1994).

¹⁹T. Mizokawa, A. Fujimori, H. Namatame, K. Akeyama, and N. Kosugi, Phys. Rev. B **49**, 7193 (1994).

²⁰A. E. Bocquet, A. Fujimori, T. Mizokawa, T. Saitoh, H. Namatame, S. Suga, N. Kimizuka, Y. Takeda, and M. Takano, Phys. Rev. B **45**, 1561 (1992).